frontiers | Frontiers in Forests and Global Change

TYPE Original Research
PUBLISHED 17 October 2023
DOI 10.3389/ffgc.2023.1233052

OPEN ACCESS

EDITED BY
Erwin Dreyer,
INRA Centre Nancy-Lorraine, France

REVIEWED BY
Pilar Pita,
Polytechnic University of Madrid, Spain
Jesús Rodríguez-Calcerrada,
Polytechnic University of Madrid, Spain

*CORRESPONDENCE
Allan Buras
✉ allan@buras.eu

RECEIVED 02 June 2023
ACCEPTED 28 September 2023
PUBLISHED 17 October 2023

CITATION
Buras A, Rehschuh R, Fonti M, Lange J, Fonti P, Menzel A, Gessler A, Rigling A, Treydte K and von Arx G (2023) Quantitative wood anatomy and stable carbon isotopes indicate pronounced drought exposure of Scots pine when growing at the forest edge.
Front. For. Glob. Change 6:1233052.
doi: 10.3389/ffgc.2023.1233052

Quantitative wood anatomy and stable carbon isotopes indicate pronounced drought exposure of Scots pine when growing at the forest edge

Allan Buras[1,2]*, Romy Rehschuh[3], Marina Fonti[4], Jelena Lange[5], Patrick Fonti[4], Annette Menzel[2,6], Arthur Gessler[4,7], Andreas Rigling[4,8], Kerstin Treydte[4] and Georg von Arx[4,9]

[1]Land Surface-Atmosphere Interactions, TU Munich, Munich, Germany, [2]Ecoclimatology, TU Munich, Munich, Germany, [3]Institute of General Ecology and Environmental Protection, Chair of Biodiversity and Nature Conservation, TU Dresden, Dresden, Germany, [4]Forest Dynamics, Swiss Federal Research Institute WSL, Birmensdorf, Switzerland, [5]Department of Physical Geography and Geoecology, Charles University, Prague, Czechia, [6]Institute for Advanced Study, Technical University of Munich, Garching, Germany, [7]Institute of Terrestrial Ecosystems, ETH Zurich, Zürich, Switzerland, [8]Forest Ecology, Institute of Terrestrial Ecosystems, ETH Zurich, Zürich, Switzerland, [9]Oeschger Centre for Climate Change Research, University of Bern, Bern, Switzerland

Climate change poses a major threat to global forest ecosystems. In particular, rising temperatures and prolonged drought spells have led to increased rates of forest decline and dieback in recent decades. Under this framework, forest edges are particularly prone to drought-induced decline since they are characterized by warmer and drier micro-climatic conditions amplifying impacts of drought on tree growth and survival. Previous research indicated that forest-edge Scots pine trees have a higher growth sensitivity to water availability compared to the forest interior with consequent reduction of canopy greenness (remotely sensed NDVI) and higher mortality rates. Yet, the underlying physiological mechanisms remain largely unknown. Here, we address this knowledge gap by comparing stable carbon isotope signatures and wood anatomical traits in annual rings of trees growing at the forest edge vs. the forest interior and between trees that either survived or died during the extreme drought of 2015. Our analyses suggest that the exposure to drought of forest-edge Scots pine likely results in a reduction of stomatal conductance, as reflected by a higher $\delta^{13}C$ of stem wood, thinner cell walls, and lower mean ring density. Moreover, we found dead trees to feature larger mean hydraulic lumen diameters and a lower cell-wall reinforcement, indicating a higher risk to suffer from cavitation. In conclusion, the typically drier micro-climatic conditions at the forest edge seem to have triggered a larger reduction of stomatal conductance of Scots pine trees, resulting in a lower carbon availability and significantly altered wood anatomical properties under an increasingly drier climate.

KEYWORDS

tree rings, hotter drought, forest microclimate, tree physiology, dieback, *Pinus sylvestris*

1. Introduction

Forest ecosystems are an essential carbon sink for climate change mitigation (Bonan, 2008). Their ability to effectively offset anthropogenic greenhouse gas emissions largely depends on their physiological integrity which has experienced a decline in recent decades due to the increasing intensity and frequency of so-called hotter droughts (Allen et al., 2010, 2015; Buras et al., 2021). As a consequence, forest ecosystems might – at least temporarily – reduce their carbon sink efficiency or even change from a carbon sink into a source, thereby exacerbating anthropogenic climate change (Ciais et al., 2005; Brienen et al., 2015; Cabon et al., 2022).

One effective means to prevent drought-induced forest decline is via forest management. This means that the ongoing climate adaptation of managed forests aims at growing tree species that are able to cope with anticipated climate in a given location as identified by empirical and mechanistic modelling (Walentowski et al., 2017; Buras and Menzel, 2019). Additional important influencing factors which can either be taken into account or actively controlled are (1) soil conditions (e.g., texture) which determine how much of the fallen precipitation is available to the plants and thus are decisive for tree-species selection (Lévesque et al., 2013; Rehschuh et al., 2017), (2) genotype affecting individual drought adaptation via specific trait expression (Seidel et al., 2016; Seidel and Menzel, 2016; Klisz et al., 2019), and (3) stand density (Kohler et al., 2010; Giuggiola et al., 2013).

Another factor affecting trees' drought vulnerability refers to variations in the forest micro-climate, which is – among others – modified by proximity to the forest edge. This is because the typically relatively milder and moister micro-climate inside the forest gradually becomes warmer and drier toward the forest edge, leading to an amplified ambient atmospheric water deficit under drought (Chen et al., 1993; Laurance and Williamson, 2001; De Frenne et al., 2021). In addition, forest fragmentation – which is strongly increasing the proportion of forest edges – has a strong effect on micro-climate and consequently forest decline (Mann et al., 2023). Particularly European forests feature a high degree of fragmentation (Estreguil et al., 2013) indicating the necessity to assess whether trees growing in proximity to the forest edge are more likely to suffer from climate-change induced decline due to a hotter and drier micro-climate. Improving our understanding on possible forest-edge drought effects is particularly important, since this micro-habitat typically is considered favorable for tree-growth due to a lower competition for light and resources when compared to the forest interior. However, with climate change triggering a higher frequency of droughts, the forest edge may turn from a favorable into an unfavorable micro-habitat, since edge-trees' stronger exposure to the macro-climate may make them more vulnerable to drought due to a relatively warmer and drier micro-climate. Indeed, Scots pine (*Pinus sylvestris* L.)–one of the most abundant and economically important tree-species in European forests – has shown (1) a higher drought sensitivity, (2) a decline in canopy greenness (as measured using remotely sensed NDVI) and growth, and (3) higher dieback frequencies at the forest edge when compared to the forest interior (Buras et al., 2018). In their study Buras et al. (2018), identified the forest edge as a potential hot-spot to adapt forests to climate change via management due to possibly arising self-amplifying feedback loops. Namely, the dieback of forest-edge trees creates new forest edges and the abruptly released trees are more likely to die during subsequent droughts, thereby causing further forest fragmentation. Consequently, improving our understanding of the observed forest-edge effects is crucial in the context of managing forests' climate resilience.

Given the isohydric strategy of Scots pine (Klein, 2014), Buras et al. (2018) hypothesized that the warmer and drier forest-edge microclimate triggers an earlier reduction of stomatal conductance and thus photosynthesis in course of the growing season when comparing forest-edge trees with the forest interior. This hypothesis was supported by the ongoing growth decline of dying forest-edge trees since the 1990ies, potentially indicating a successive carbon depletion due to a shortage of photo-assimilates (Buras et al., 2018). However, this interpretation was solely based on tree-ring widths and derived basal-area increments, which do not allow for direct inference on tree physiology. Here, stable carbon isotope measurements may shed further light on the underlying mechanisms of growth decline and dieback, since they render a well-established proxy for intercellular CO_2-concentrations in leaves and thus indirectly for water-use efficiency, stomatal conductance, and assimilation rate (Farquhar et al., 1982; Klein et al., 2013). In a similar manner, a lower availability of photo-assimilates due to a more prominent drought exposure might result in thinner cell walls, as was reported for Scots pine in dry inner-alpine valleys (Eilmann et al., 2009). Moreover, to improve water transport capacities, Scots pine may adapt to dry conditions by widening its lumina as hypothesized by Eilmann et al. (2009) based on corresponding observations.

An unresolved question from Buras et al. (2018) refers to the observed patchy dieback patterns, with neighboring live and dead individuals as previously also observed for several species (Hentschel et al., 2014; Cailleret et al., 2017). Potential causes of such individual responses could be related to hydraulic properties, structural overshoot, i.e., an undersupplied water demand under drought caused by a too high leaf area in relation to the root system which is induced by previously beneficial environmental conditions (e.g., Jump et al., 2017), competition and soil conditions (Klesse et al., 2022), root architecture, and secondary pathogens. Here, structural properties of the xylem related to hydraulic safety could render a promising avenue for identifying potential pre-disposing factors for individual tree dieback. Earlier studies have shown that the proportions of cell-wall thickness and lumen diameter can be combined into a biomechanical metric, the so-called cell-wall reinforcement index, which describes the risk of cell implosion (Hacke et al., 2001). Although conifers generally operate at much higher water potential than would be required to collapse the tracheids based on the cell-wall reinforcement index, this metric is strongly correlated with measured hydraulic safety or P_{50}, i.e., the water potential at which 50% of xylem conductivity is lost due to cavitation (Hacke et al., 2001). In addition, there is also empirical evidence linking this metric and other structural-functional xylem traits to drought and tree vitality or dieback (Eilmann et al., 2009; Rosner et al., 2016; Guérin et al., 2020). Thus, investigating hydraulic properties as inferred from the xylem anatomy renders an additional and relatively easy-to-assess promising avenue for identifying potential pre-disposing factors for individual tree dieback.

Under this framework, we here deploy quantitative wood anatomy (QWA, i.e., metrics related to cell-wall thickness and lumen size) and tree-ring stable carbon isotope ratios ($\delta^{13}C$) from live vs. dead trees at the forest edge vs. live trees in the forest interior to shed light on the physiological mechanisms causing growth decline and dieback of

Scots pine from hotter drought at the forest edge. Time series of QWA traits allow for inferring on hydraulic properties of the xylem at intra-annual resolution and consequently may identify differing hydraulic properties among the investigated tree categories. In contrast, tree-ring $\delta^{13}C$ time series are considered proxies for intrinsic water use efficiency and stomatal conductance (Klein et al., 2013). Although $\delta^{13}C$ time series derived from woody tissue cannot be considered a direct measure of whole-tree carbon fluxes at the time of wood-formation (e.g., due to mobilization of non-structural carbohydrates), they may nevertheless provide further insights into a differing exposure to drought between edge and interior trees. Combining these two complementary methodological approaches and based on existing knowledge mentioned above, we hypothesize:

> *H1*: Given their stronger exposure to high VPD and low soil-water potentials, which for an isohydric species such as Scots pine would result in a more frequent reduction of stomatal conductance, forest-edge trees and in particular trees which died during the extreme drought of 2015 are characterized by a weaker discrimination against ^{13}C in comparison to the forest interior which will be reflected in higher (i.e., less negative) $\delta^{13}C$ values of stem wood.
>
> *H2*: Given a stronger exposure to drought, annual variability of $\delta^{13}C$ in the stem wood is more strongly linked to atmospheric drought conditions for trees growing at the forest edge and particularly for dead forest-edge trees.
>
> *H3*: Since a more frequent exposure to, behind drought conditions would result in a lower availability of photo-assimilates for xylem formation in an isohydric species as Scots pine (H1), we hypothesize mean ring density and cell-wall thickness to be lower at the forest edge and particularly for dead forest-edge trees in comparison to the forest interior.
>
> *H4*: In case of a lower availability of photo-assimilates for xylogenesis caused by a higher exposure to drought (H1, H3) edge trees and in particular dead forest-edge trees may adjust their anatomy by forming larger lumina to facilitate water transport. If so, this would translate into larger mean hydraulic diameter which in combination with the hypothesized lower cell-wall thickness (H3) would result in a lower cell-wall reinforcement at the forest edge.

2. Materials and methods

2.1. Sample selection

To obtain QWA and $\delta^{13}C$ data, we resampled the Scots pine increment cores taken in 2016 at one of the five study sites presented in Buras et al. (2018), namely the site 'Maisenlach' which is located south of the city of Schwabach in Franconia, Germany (lon: 11.029°, lat: 49.305°, WGS 84). Among the 5 sites, we specifically selected this site due to its south-facing forest edge and thus strongest micro-climatic effects at the edge (Chen et al., 1993; Matlack, 1993; Young and Mitchell, 1994) as well as the largest sample size of available increment cores (see Buras et al., 2018). Two other stands from Buras et al. (2018) also featured south-facing edges, but the site 'Neustadt an der Aisch' represents a small forest patch with overlapping effects from different forest edges, while the site 'Hessdorf' was characterized by a fragmented forest-edge which may cause additional modifications to the forest microclimate.

At the time of sampling the 'Maisenlach' forest stand was dominated by Scots pine with a mean age of 102 ± 17 years. After the extreme drought of 2015, a remarkable tree canopy browning and dieback of individual trees at the forest edge was observed in spring 2016, which lead to the investigations presented in Buras et al. (2018). Considering tree dimensions, diameter at breast height and remotely sensed canopy area statistically belonged to the same distribution ($p > 0.05$), while tree height was significantly ($p < 0.001$) lower at the forest edge (see Figure 2 in Buras et al., 2018). Indexed ring-width series from the 'Maisenlach' featured a high growth synchronicity as indicated by an average Gleichläufigkeit (glk, see Eckstein and Bauch, 1969; Buras and Wilmking, 2015) of 0.67, a mean inter-series correlation (rbar) of 0.47, and an expressed population signal of 0.98 (EPS, see Wigley et al., 1984; Buras, 2017). The forest soil was characterized as a stagnic Gleysol.

To identify the most-suitable tree individuals for our purpose, we utilized the initially obtained 46 individual ring-width series consisting of 8 dead edge trees, 18 live edge trees, and 20 live interior trees. The ring-width series were detrended into ring-width indices (RWI) using an autoregressive model (known as pre-whitening) to emphasize the high-frequency growth variations representative of the climate signal in ring-width variations. Subsequently, we applied a Principal Component Gradient Analysis over the common overlap period 1942–2011 (PCGA, Buras et al., 2016). PCGA allows for identifying ecological gradients within populations of tree-ring samples that are expressed in subtle variations in RWI series (Buras et al., 2016; Rehschuh et al., 2017). This population-inherent gradient was used to identify each five specimens of each of the three categories (dead vs. live at the edge vs. interior trees) within the population gradient. Here, we aimed at selecting specimens which featured extreme PCGA-ranks along the population-inherent gradient. This was done to particularly emphasize on growth patterns representative of the three different categories. However, since some of the samples could not be used for QWA assessments due to suboptimal wood quality of the increment cores (e.g., wood decay and/or cracks), we slightly modified the statistical selection by selecting alternative individuals along the population gradient. Nevertheless, the eventually selected samples represent statistically significantly differing growth patterns between edge and interior trees as indicated by a pairwise Wilcoxon rank-sum test (see Supplementary Figure S1). To confirm that these subsamples represent the corresponding tree categories, we computed inter-series correlations and glk between subsample chronologies and their corresponding counterpart including all trees from a specific tree category. Since all correlations between subsample and counterpart chronologies were larger than 0.88 ($p < 0.001$) and glk values were larger than 0.82 ($p < 0.001$), we considered the subsample chronologies representative of the three tree categories. Furthermore, we tested whether diameters at breast height of the three subsample categories belonged to the same population using a pairwise Wilcoxon rank-sum test which returned non-significant ($p > 0.05$) results for all three pairwise comparisons. For each of these altogether 15 trees, we further utilized (1) detrended RWI (see above), (2)

basal-area increments (BAI) based on ring-width and measured diameters at breast height as a measure of secondary growth (bai.out function in the 'dplR' R-package), (3) various QWA traits (see section 2.2) at intra-annual resolution as well as (4) $\delta^{13}C$ values (see section 2.3) at annual resolution to address the above mentioned four hypotheses H1–H4.

2.2. Quantitative wood anatomy measurements

The cell anatomical measurements were performed on cross-section images from microslides obtained from the outmost 20 annual rings of each selected radial stem core using standard protocols (Gärtner and Schweingruber, 2013; von Arx et al., 2016). Resin was extracted using a Soxhlet apparatus for 24 h. After that, cores were split into 2–3 cm long segments, embedded in paraffin, and cut in 12-µm-thick transverse sections using a rotary microtome (Leica RM2245, Leica Biosystems, Nussloch, Germany). Sections were stained with a 1:1 Safranin-Astrablue solution and permanently mounted on glass slides with Euparal (Carl Roth, Germany). For each slide, digital images were taken using a slide scanner (Axio Scan Z1, Zeiss, Germany). ROXAS software (von Arx and Carrer, 2014) combined with Image-Pro Plus (Media Cybernetics, Rockville, MD, USA) was used to semi-automatically identify tracheids from the anatomical images (von Arx et al., 2016; Prendin et al., 2017). Tracheid identification and tree-ring dating was additionally quality-checked by an experienced operator. Cell lumen area and cell wall thickness of each tracheid, together with its positional information within the dated tree ring were eventually obtained.

The following xylem anatomical traits were subsequently calculated from the initial cell measurements and integrated at the ring level for early- and latewood separately. The earlywood-latewood boundary was defined by applying the common threshold of a Mork value of 1 (Denne, 1989). Although the ROXAS output provides a multitude of wood anatomy traits, we focused on the mean cell-wall thickness (average of radial and tangential walls) of the earlywood and latewood, the anatomically derived mean ring density, i.e., a proxy for annually resolved wood density on a relative scale that is calculated as the ratio between cell wall and whole-cell area and then multiplied by 1.5 g/cm^3 (Björklund et al., 2017, 2019), the earlywood mean hydraulic diameter Dh according to Tyree and Zimmermann (2002), and the early- and latewood cell-wall reinforcement (t/b)^2 of the entire ring according to Hacke et al. (2001), where t is the double-cell wall thickness and b is the lumen diameter of a given tracheid measured perpendicularly to the double-cell wall, thus expressing the implosion safety that is strongly correlated with hydraulic safety or P_{50} (Hacke et al., 2001). We are well aware that some of these metrics are not independent from each other (e.g., cell-wall thickness and mean ring density, Dh and cell-wall reinforcement). Nevertheless, we decided for evaluating all of them, since their combined interpretation allows for a more comprehensive picture of possible wood-anatomical differences between the investigated groups and in context of our hypotheses. Eventually, the time series were truncated to the period 1998 to 2015 to assure that each of the three categories was represented by at least three individuals in a given year (individual years from individual samples were excluded due to micro-cracks).

2.3. Cellulose extraction and isotope ratio mass spectrometry

For $\delta^{13}C$ analysis of cellulose, tree rings of the last 15 years (2001–2015) of dead and live edge and living interior trees ($n = 5$, respectively) were analyzed. Approximately 15 mg of chopped material per tree ring was extracted in Teflon filter bags (Fiber Filter Bags F57, Ankom Technology, Macedon, NY, USA) using 5% NaOH at 60°C for 2 h to remove hemicellulose (Galiano et al., 2017); this procedure was carried out twice. In the following, samples were soaked in 7% acidified $NaClO_2$ (using 96% acetic acid) at 60°C for 20–40 h to fully remove resin and lignin. The extraction solution was renewed every 10 h. Lastly, Teflon filter bags were oven-dried for 12 h at 60°C and samples removed. Samples were then soaked in deionized water for several hours and homogenized using an Ultrasonic transducer (Laumer et al., 2009). Samples were finally freeze-dried for 36 h.

To determine the isotopic composition, *ca.* 1 mg of homogenized cellulose material was weighed into tin capsules. Subsequently, samples were combusted to CO_2 in an elemental analyzer (EA1110 CHN; Carlo Erba, Milan, Italy) linked to an isotope ratio mass spectrometer (Delta XL; Thermo Scientific, Bremen, Germany). Laboratory and international standards with known $\delta^{13}C$ were used for calibration, resulting in a precision of 0.2‰.

The $^{13}C/^{12}C$ ratios are expressed in δ notation (‰) relative to the international standard Vienna Pee Dee Belemnite (VPDB; $R_{Standard} = 0.0111802$):

$$\delta^{13}C = \left(\frac{R_{sample}}{R_{standard}} - 1 \right) \cdot 1000‰ \quad (1)$$

Since we were only interested in relative difference of $\delta^{13}C$ among the different tree groups investigated, $\delta^{13}C$ of wood cellulose was not corrected for atmospheric $\delta^{13}C$ to account for the increase in ^{13}C-depleted CO_2 emissions with industrialization (Loader et al., 2007), since a corresponding correction would not change the relative differences due to a common correction procedure. Altogether, the sampled $\delta^{13}C$ thus represent the annual isotopic signal integrated over a whole growing season that result from the transport of photo-assimilates from the canopy to the sinks (in case of our samples secondary wood formation) via the phloem. We therefore consider them as proxies of assimilation rates, intrinsic water-use efficiency and stomatal conductance at the canopy scale (Klein et al., 2013).

2.4. Statistical analyses

To assess whether the sample selection represents statistically differing population samples (and thus confirm representativity of the groups presented in Buras et al., 2018), we re-ran a PCGA on the subset of the 15 RWI time series. Subsequently, we computed group-wise master-chronologies, i.e., for each parameter and group we computed the corresponding annual mean value to represent

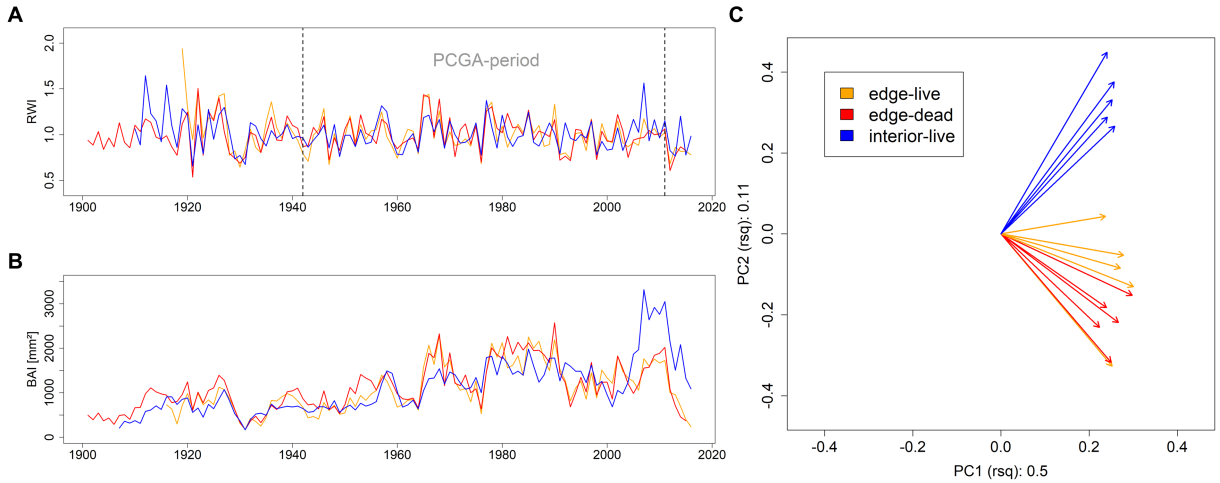

FIGURE 1
Indexed ring-widths RWI **(A)**, basal-area increments BAI **(B)**, and PCGA-loadings derived from RWI **(C)** of the 15 selected individuals for anatomy and isotope analyses and colored according to their group-association (orange, edge live; red, edge dead; blue, interior live). Values on the axes labels of panel **(C)** refer to the explained variance (r^2) of the corresponding principal component.

group-specific variations of tree-ring parameters. These chronologies were then compared against each other in context of our formulated hypotheses. Since the data were partly non-normally distributed (as tested for using Shapiro–Wilk normality test), we consistently applied non-parametric tests, i.e., Wilcoxon rank-sum test and Spearman's rank correlation.

To obtain a general overview on differences in growth patterns (RWI) and growth levels (BAI), we firstly visually compared the RWI- and BAI- master chronologies of the three different categories. Moreover, we for each of the three categories calculated glk, rbar, and EPS from individual series as a measure of growth synchronicity and statistically compared glk and inter-series correlations among the three categories using a pairwise Wilcoxon rank sum test.

In terms of addressing H1, we assessed the averaged $\delta^{13}C$ time series (i.e., category-specific chronologies) for significant differences between the three groups using a paired (by year), pairwise Wilcoxon rank-sum test. Here, a significant result indicates systematically different yearly values in the compared chronologies. In case H1 were true, forest interior trees should feature significantly lower $\delta^{13}C$ values compared to forest-edge trees, with dead forest edge trees featuring highest $\delta^{13}C$ values, i.e., lowest photosynthetic discrimination against ^{13}C.

To address H2, we correlated $\delta^{13}C$ time series with the standardized precipitation evapotranspiration index (SPEI, Vicente-Serrano et al., 2009) as retrieved from the corresponding grid-cell of CRU monthly temperature and precipitation data (version 4.06; Harris et al., 2020). The SPEI represents the locally standardized climatic water balance (P-PET; Thornthwaite, 1948) which was shown to indicate plants sensitivity to water supply during the growing season (e.g., Buras et al., 2018). To represent water availability over the full growth period, we integrated SPEI over 9 months representing January–September SPEI for each year. We included the water balance in late winter/ early spring (i.e., January, February, March) since this better reflects soil water availability at the onset of growth. The January–September SPEI time series was finally correlated with each of the three $\delta^{13}C$ chronologies. These correlations allow for directly addressing H2, which refers to the coupling of tree-ring $\delta^{13}C$ with plant water availability as reflected by January–September SPEI. That is, in case H2 were true, the obtained correlations should be highest for dead edge trees, followed by live edge trees and live interior trees, reflecting a higher frequency of reduced stomatal conductance induced by low soil water potentials at the forest edge and in particular for dead edge trees.

Regarding H3, we statistically compared category-specific chronologies of earlywood and latewood cell-wall thickness as well as mean ring density using paired (by year) pairwise Wilcoxon rank-sum tests. In case H3 were true, all three traits should feature lower values at the forest edge in comparison to the forest interior, potentially reflecting a lower availability of photo-assimilates for xylem formation.

Finally, to address H4 we statistically compared category-specific chronologies of the mean hydraulic diameter as well as the cell-wall reinforcement as proxies for tracheid-implosion safety using paired (by year) pairwise Wilcoxon rank-sum tests. In case H4 were true, dead trees should feature statistically higher mean hydraulic diameters and lower cell-wall reinforcement compared to live trees.

All analyses were conducted in 'R' (version 4.2.2; R Core Team, 2022) extended for the packages 'SPEI' (Beguería and Vicente-Serrano, 2013), 'dplR' (Bunn, 2008), and 'dendRolAB' (Buras, 2022).

3. Results

According to PCGA, RWI expressed significantly differing high-frequency growth variations among the three groups (Figure 1C). This was reflected in clearly different high-frequency growth patterns (Figure 1A). With regards to BAI, edge trees featured higher absolute growth rates compared to interior trees in the pre-1990 period. At the onset of the 1990ies, edge trees expressed a remarkable growth reduction which was not seen in forest interior trees. In the mid 1990ies, edge trees featured growth-levels equal to those expressed by interior trees. Finally, the growth of edge trees was overtaken by interior trees in 2006 (Figure 1B).

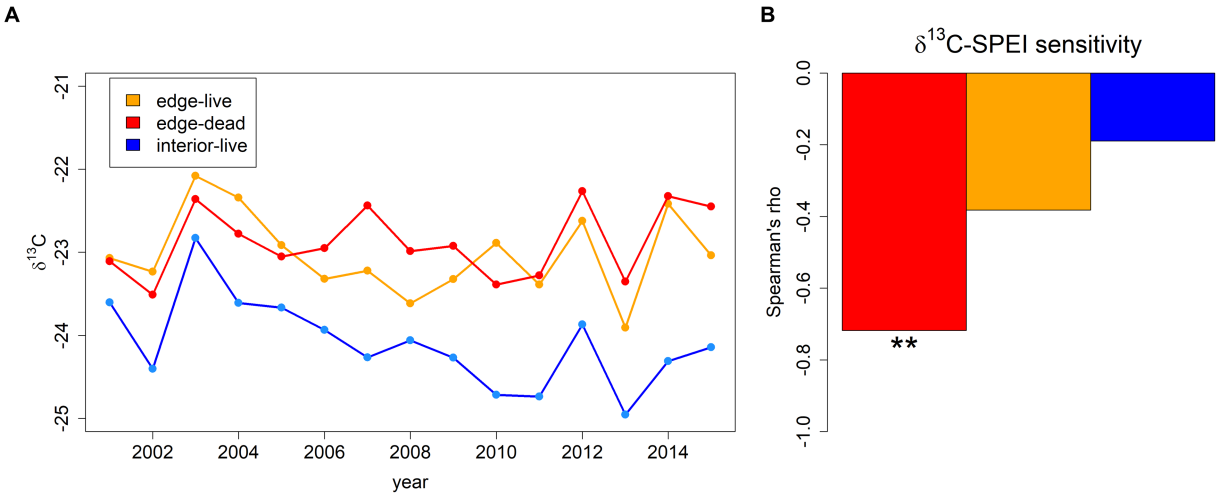

FIGURE 2
$\delta^{13}C$ time series **(A)** averaged per year over all individuals belonging to one of the three sub-groups, i.e., edge live (orange), edge dead (red), and forest interior live (blue). Spearman's rank correlation coefficient rho of corresponding time series with January–September SPEI integrated over 9 months **(B)**. Asterisks in panel **(B)** indicate significance ($p < 0.01$) of Spearman's rho. Boxplots indicating the absolute range of values depicted in panel **(A)** are shown in Supplementary Figure S2.

At the forest edge, glk featured 0.65 for both live and dead trees, while rbar was 0.47 and 0.48 for live and dead trees, respectively. In the forest interior, glk featured 0.75 and was significantly higher compared to the forest edge (test against both live and dead edge trees $p < 0.01$). Also, rbar was higher in the forest interior (0.59) with individual inter-series correlations being significantly different between interior and live edge trees ($p = 0.03$).

$\delta^{13}C$ chronologies indicated systematically and significantly higher values and thus a lower discrimination against ^{13}C at the forest edge in comparison to the forest interior (H1: $p < 0.001$; Figure 2A; Table 1). In comparison, the differences between live and dead trees' $\delta^{13}C$ chronologies at the forest edge were not significant ($p = 0.21$; Table 1). However, dead edge trees had a much stronger and significant ($p < 0.01$) correlation with January–September SPEI in comparison to live edge ($p = 0.16$) trees and in particular interior trees ($p = 0.49$; H2; Figure 2B; Table 1).

Regarding the quantitative wood anatomy traits, significant differences were found between edge and interior trees and also between live and dead edge trees for most of the investigated parameters (Figure 3; Table 1). Edge trees had significantly thinner latewood cell walls ($p < 0.001$ for both live and dead edge trees vs. interior trees) with a pronounced decline observed for dead edge trees from the year 2012 onwards (H3; Figure 3A). The difference between live and dead edge trees, however, was not significant ($p = 0.13$). Earlywood cell-wall thickness differed significantly among all groups (H3; $p < 0.001$ for all pairwise comparisons) with thinnest cell walls being observed for dead edge trees (Figure 3B). The patterns observed for cell-wall thickness were paralleled by mean ring density (Figure 3C), i.e., ring density differed significantly among the three groups (H3; $p < 0.001$ for both pairwise tests between edge and interior trees and $p < 0.01$ for the comparison between live and dead edge trees, see Table 1) and was lowest for dead edge trees. Earlywood mean hydraulic diameter (Figure 3D) differed significantly among all three groups (H4; $p < 0.05$ for live vs. dead edge trees and between live edge vs. interior trees, $p < 0.01$ for dead edge vs. interior trees, see Table 1). Over the period 2003 through 2012, dead edge trees had a systematically higher earlywood mean hydraulic diameter compared to live trees. Interestingly, earlywood mean hydraulic diameters abruptly and strongly declined for both live and dead edge trees in the year 2014. The cell-wall reinforcement differed among the groups (H4). Yet, differences were more pronounced in the latewood compared to the earlywood (Figures 3E,F; Table 1). That is, for the earlywood, only the pairwise comparison between dead edge and interior trees was significant ($p = 0.01$) while for the latewood, all comparisons were highly significant ($p < 0.001$) with dead edge trees featuring lowest values in both early- and latewood.

4. Discussion

The presented analyses based on $\delta^{13}C$ and quantitative wood anatomy traits statistically support the initially posed hypotheses. In the following, we elaborate on each of the findings in context of the formulated hypotheses.

4.1. Higher $\delta^{13}C$ at the forest edge

Regarding H1, we found significantly higher $\delta^{13}C$ values for forest-edge trees but no significant differences between live and dead edge trees. As initially hypothesized, we interpret this finding as a systematically earlier reduction of stomatal conductance of forest-edge trees compared to forest-interior trees under dry conditions. Photosynthetic carbon isotope fractionation and thus the resulting $\delta^{13}C$ in the assimilates is in a first approximation proportional to the relationship between the leaf internal (C_i) and the ambient CO_2 (C_a) concentration (Farquhar et al., 1982), which is in turn determined by the assimilation rate on the one hand and by stomatal conductance on the other hand (Gessler et al., 2018). Any increase in $\delta^{13}C$ might thus

TABLE 1 Overview on the applied statistical tests which refer to paired pairwise Wilcoxon rank-sum tests (H1, H3, and H4) and Spearman's rank correlations (H2).

Hypothesis	Metric	Groups (compared)	Mean (difference ± se)	Value of *p*
H1	**$\delta^{13}C$**	**Edge-live vs. interior**	**1.1 ± 0.11**	**<0.001**
		Edge-dead vs. interior	**1.2 ± 0.13**	**<0.001**
		Edge-live vs. edge-dead	0.15 ± 0.11	0.21
H2	**$\delta^{13}C$**	Interior	0.18[1]	0.49
		Edge-dead	**0.72**[1]	**<0.01**
		Edge-live	0.38[1]	0.16
H3	**CWT_{LW}**	**Edge-live vs. interior**	**0.42 ± 0.10**	**<0.01**
		Edge-dead vs. interior	**0.68** ± 0.15	**<0.001**
		Edge-live vs. edge-dead	0.16 ± 0.09	0.13
H3	**CWT_{EW}**	**Edge-live vs. interior**	**0.32 ± 0.04**	**<0.001**
		Edge-dead vs. interior	**0.42 ± 0.05**	**<0.001**
		Edge-live vs. edge-dead	**0.10 ± 0.02**	**<0.001**
H3	**RD**	**Edge-live vs. interior**	**0.06 ± 0.008**	**<0.001**
		Edge-dead vs. interior	**0.08 ± 0.007**	**<0.001**
		Edge-live vs. edge-dead	**0.02 ± 0.005**	**<0.01**
H4	**Dh_{EW}**	**Edge-live vs. interior**	**1.04 ± 0.42**	**0.03**
		Edge-dead vs. interior	**1.88 ± 0.46**	**<0.01**
		Edge-live vs. edge-dead	**0.84 ± 0.29**	**0.03**
H4	**CWR_{LW}**	**Edge-live vs. interior**	**0.29 ± 0.06**	**<0.001**
		Edge-dead vs. interior	**0.46 ± 0.05**	**<0.001**
		Edge-live vs. edge-dead	**0.18 ± 0.03**	**<0.001**
H4	**CWR_{EW}**	Edge-live vs. interior	0.005 ± 0.003	0.18
		Edge-dead vs. interior	**0.009 ± 0.002**	**<0.05**
		Edge-live vs. edge-dead	0.004 ± 0.002	0.11

[1]Values refer to Spearman's rho and are thus reported without standard error.
Significant results are indicated in bold font. CWT, cell-wall thickness; RD, ring density; Dh, hydraulic diameter; CWR, cell-wall reinforcement. EW: earlywood and LW: latewood.

be due to a higher assimilation rate or a lower stomatal conductance since they both decrease C_i and thus photosynthetic carbon isotope fractionation. The observed reduction of tree growth at the forest edge since approx. 1990 (Figure 1) as well as the lower cell-wall thickness (Figure 3) suggests that the higher $\delta^{13}C$ values of edge trees are an indication of reduced stomatal conductance and not of higher assimilation rates. It may be argued, that edge trees are comparably less shaded resulting in a higher assimilation rate. However, Brandes et al. (2006) showed that there is no shading effect on $\delta^{13}C$ of assimilates in Scots pine. Moreover, the study area of Franconia, Germany, has experienced an increasingly drier climate since 1990 (Buras et al., 2018; Supplementary Figure S4), which coincides with a lower growth of forest-edge trees compared to forest-interior trees since then (Figure 1B) and supports the assumption of a drought-induced reduction of stomatal conductance as the primary reason for the observed differences in $\delta^{13}C$ (Figure 2A). Namely, due to the more frequent reduction of stomatal conductance, forest-edge trees featured a relatively lower carbon assimilation, which likely resulted in the observed lower growth values since 1990. Another possible explanation for reduced growth rates at the forest edge is a possibly enhanced respiration at the forest edge. However, since absolute growth at the forest edge declined in the 1990ies (Figure 1B), i.e., under an increasingly drier climate in the region (Buras et al., 2018), it seems more likely that the relatively isohydric Scots pine specimens studied here, reduced stomatal conductance at the cost of photosynthesis. This interpretation is supported by previously published research. For instance, Pellizzari et al. (2016) reported a higher $\delta^{13}C$ of declining Scots pine individuals when compared to neighboring non-declining individuals. Another study reported a rapid decrease of $\delta^{13}C$ after irrigating Scots pine in a dry inner-alpine valley which coincided with increased growth rates (Eilmann et al., 2010). In our interpretation, it is yet important to mention that differences in rooting depth and thus soil-water access may affect the observed differences in $\delta^{13}C$ of edge and interior trees. Unfortunately, corresponding data was not available wherefore this hypothetical influencing factor remains subject to further investigation. We want to stress, that $\delta^{13}C$ is not a direct measure of whole-tree carbon fluxes at the time of wood formation (e.g., due to the mobilization of non-structural carbohydrates) wherefore there might be additional factors (e.g., carry-over effects) determining the variability of $\delta^{13}C$ time-series. Yet, since our results are in line with observations for Scots pine in other investigations (Eilmann et al., 2010; Pellizzari et al., 2016) and given the observed positive relationship between $\delta^{13}C$ and January–September SPEI, it seems likely that stomatal conductivity

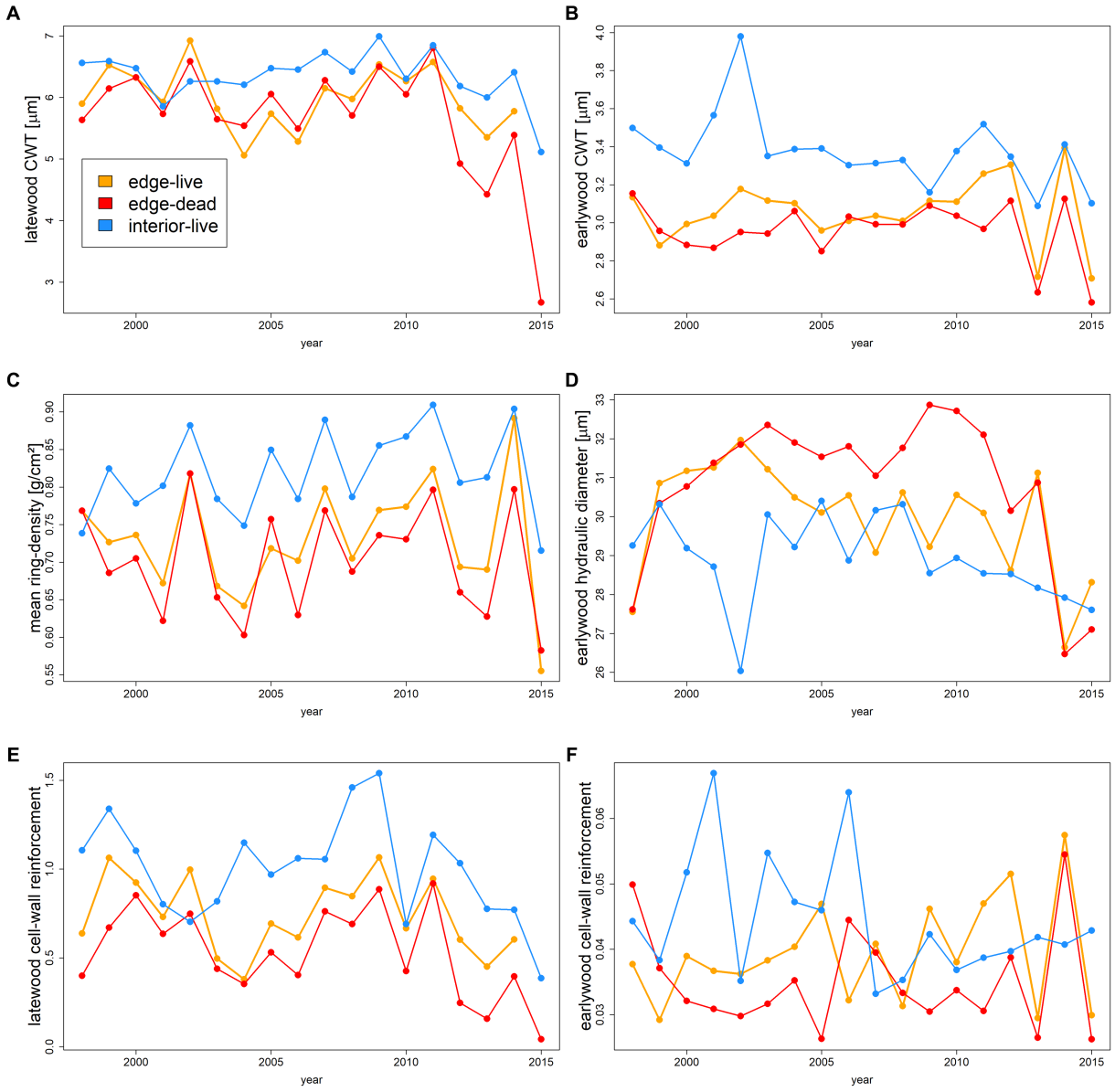

FIGURE 3
Time series of quantitative wood anatomy traits averaged per year over all individuals belonging to one of the three sub-groups, i.e., edge live (orange), edge dead (red), or forest interior live (blue). Presented traits refer to latewood cell-wall thickness **(A)**, earlywood cell-wall thickness **(B)**, mean ring density **(C)**, earlywood mean hydraulic diameter **(D)**, latewood cell-wall reinforcement **(E)**, and earlywood cell-wall reinforcement **(F)**. Boxplots indicating the absolute range of values depicted in all panels are shown in Supplementary Figure S3.

and intrinsic water-use efficiency are to a high degree reflected by our measurements.

A potentially more frequent reduction of stomatal conductance at the forest-edge compared to the forest-interior as suggested by our results is likely caused by the different micro-climatic conditions. First of all, the forest edge generally features a micro-climate more representative of open land, which has been reported to be warmer and drier particularly under drought (Chen et al., 1993; Bonan, 2008; De Frenne et al., 2021; Meeussen et al., 2021). Secondly, forest-edge trees feature a higher leaf-area index due to more leaves at lower branches compared to the forest interior despite a similar canopy area (Sherich et al., 2007; Buras et al., 2018) potentially causing higher water losses via transpiration. In other words, the higher leaf-area index due to more favorable light conditions at the forest edge results in an unsupplied water demand of the canopy under drought, which can be interpreted as structural overshoot (Jump et al., 2017). Under drought, these two effects in combination result in a faster soil water depletion and thus more negative soil water potentials in comparison to the forest interior. Relatively isohydric tree species – such as the here investigated Scots pine – reduce stomatal conductance under increasingly negative water potentials (Klein, 2014). In conclusion, the physiological drought-response of edge trees did not only result in relatively higher $\delta^{13}C$ values but also reduced secondary growth in comparison to forest interior trees (see also relative temporal

changes of BAI in Figure 1). The previously shown higher SPEI-sensitivity of RWI derived from forest-edge Scots pines in comparison to the forest interior (Buras et al., 2018) supports this interpretation. That is, the higher SPEI-sensitivity of forest-edge trees reflects a stronger coupling to soil-water conditions compared to the forest interior, which is in line with the observed ongoing growth decline at the forest edge since the 1990ies under an increasingly drier climate. Further support to this interpretation comes from Buras et al. (2018), who reported significantly lower latewood-earlywood ratios at the forest edge, potentially indicating resource shortage in the typically warm and dry later part of the growing season. The higher sensitivity of $\delta^{13}C$ to January–September SPEI in dead trees provides further support to this interpretation and supports H2. That is, the tree-ring $\delta^{13}C$ variations were strongly negatively correlated to January–September SPEI in dead edge trees but to a lesser extent in live edge trees. Combined with the higher $\delta^{13}C$ values at the forest edge this suggests particularly reduced ^{13}C discrimination in dry years. Again, this can be interpreted as a faster drying of the forest-edge microclimate in dry years, causing an earlier reduction of stomatal conductance and therefore lower discrimination against ^{13}C. The observed much stronger link between $\delta^{13}C$ and water availability in dead edge trees (Spearman's rho = 0.72) compared to live edge trees (rho = 0.38) possibly indicates that these trees were more constrained by the dry forest-edge microclimate.

Possible factors causing a drier micro-climate for dead trees in comparison to live trees at the forest edge refer to differences in soil properties, leaf-area index, and tree exposure to macro-climate. Previous studies have shown that plant available water capacity modulates the coupling of tree growth with soil-water availability (e.g., Lévesque et al., 2013; Rehschuh et al., 2017). Theoretically, small-scale variations of soil texture – governing plant available water capacity – may to some degree explain the observed individual differences between the investigated trees concerning detrimental effects that likely were caused by a higher exposure to drought. Moreover, belowground competition for water resources may cause trees' differing drought-sensitivity. That is, trees suffering a stronger belowground competition, e.g., by the roots of understory shrubs or neighboring trees are more likely to experience water shortage in dry years (Giuggiola et al., 2016, 2018). Besides soil conditions, exposure of individual trees to the macro-climate can also lead to a higher drought-induced mortality risk. During drought, trees whose crowns are more exposed to the macro-climate suffer from higher canopy temperatures, higher turbulence, and in combination a higher vapor pressure deficit (Grote et al., 2016). Another important factor is leaf-area index, which tends to be larger for exposed trees, since lower branches receive more sunlight and thus retain a higher amount of foliage (Sherich et al., 2007). If assuming similar stomatal conductance under well-watered conditions early in the growing season, water-loss via transpiration is higher in exposed trees, resulting in earlier drought stress compared to less exposed individuals. The observation of significantly lower glk and inter-series correlation of forest-edge trees compared to the forest interior indicates more heterogeneous tree-responses to environmental conditions at the forest edge. Unfortunately, we neither recorded understory vegetation nor did we analyze soil samples or tree exposure to macro-climate to investigate these possible explanations, which is why these hypothetical explanations should be taken into consideration in future investigations. We can also not exclude genetic differences among live and dead individuals, which are also known to potentially affect mortality patterns (Hentschel et al., 2014).

4.2. Differences in wood anatomical traits

The observed lower cell-wall thickness and consequently mean ring density of edge trees supports H3. This finding likely indicates a lower availability of photo-assimilates for xylem formation during the period of investigation (i.e., at least since 1998) and is in line with the interpretation of photosynthetic downregulation in response to the reduction of stomatal conductance during drought as a dominant physiological agent of the observed forest-edge effects (H1 and H2). Our interpretation is in line with a study from Central Switzerland, in which the authors reported a temporarily reduced earlywood cell-wall thickness for Scots pine individuals that had experienced an abrupt reduction in water availability due to the drainage of an adjacent water-channel (Eilmann et al., 2009). In their study, the authors also interpreted reduced cell-wall thickness as a reduced carbon investment under drought. Further support to this interpretation comes from a drought-related study on *Pinus nigra* in Northern Italy (Petrucco et al., 2017), a drought experiment on *Pinus edulis* in New Mexico (Guérin et al., 2020), and a study focusing on drought-induced mortality of *Pinus canariensis* (López et al., 2021). It is important to stress, that trees growing under relatively drier conditions typically adjust to lower stem-water potentials by growing stronger tracheids with thicker cell walls (Hacke and Sperry, 2001) which is in contrast to our finding. We see this discrepancy between our findings and existing theory as further support to our interpretation, namely that the observed thinner cell walls at the forest edge reflect a drought-induced lower availability of photo-assimilates as also reported in other studies dealing with drought effects in pine species (Eilmann et al., 2009; Guérin et al., 2020; López et al., 2021).

Under this framework, the fact that earlywood cell-wall thickness was systematically and significantly lower for dead compared to live edge trees may further support the micro-environment hypothesis formulated in context of $\delta^{13}C$ and H2. That is, a soil texture causing a lower water-holding capacity and increased water competition, of dead trees may also result in a reduced cell-wall thickness compared to neighboring trees, given a reduced production of photo-assimilates. Yet, this hypothetical interpretation needs further support by additional investigations based on a higher replication of dead and live individuals and a minute investigation of individual trees' macro-climatic exposure and soil conditions.

Finally, our results support H4. That is, edge trees and in particular dead trees featured a systematically and significantly higher earlywood mean hydraulic diameter. In combination with the observed lower earlywood cell-wall thickness, this results in a lower cell-wall reinforcement and thus hydraulic safety in edge vs. interior trees. Again, this finding is in line with Eilmann et al. (2009) who reported a significantly higher lumen diameter (and thus mean hydraulic diameter) of Scots pine after the cessation of irrigation from which they concluded a higher implosion risk. Similar observations were made for *Pinus edulis*, which featured a lower tracheid-implosion safety in a drought experiment (Guérin et al., 2020). The observed larger mean hydraulic

diameter may be interpreted as a morphological adaption to resource scarcity under drought-prone conditions at the forest edge. That is, comparably less photo-assimilates are invested to maintain hydraulic conductivity high enough to supply crowns with water rather than spending more photo-assimilates to build more cells with a higher cell-implosion safety (Sperry, 2003; Prendin et al., 2018; Guérin et al., 2020). The observation, that differences between the investigated tree categories was most prominent in the latewood supports this interpretation. Namely, latewood is typically formed in summer and thus at a time when photo-assimilation frequently is reduced due to drought-stress due to a high atmospheric water demand. As a consequence, edge trees which may experience an amplified summer drought may feature thinner cell walls and larger lumen diameters to favor water transport. In addition, larger canopy volumes resulting from higher light availability and reduced competition at the forest edge might need to be supplied with relatively more water than the canopy of interior trees (Sherich et al., 2007), potentially amplifying this hydraulic adjustment, which however, comes at the cost of an increased risk of implosion (Hacke et al., 2001). In fact, Hacke et al. (2001) have shown a clear relationship between cell-wall reinforcement and P_{50}, i.e., the xylem water potential at which 50% loss of conductivity occurs due to cavitation. Thus, with a lower cell-wall reinforcement, a less negative water potential is needed for 50% cavitation. Given this negative relationship between cell-wall reinforcement and cavitation risk, we interpret the significantly lower cell-wall reinforcement at the forest edge as a higher probability of cavitation, which under an increasingly drier climate may result in vitality decline and tree dieback.

The observed larger hydraulic diameters at the forest edge may theoretically also result from larger tree heights. At breast height taller trees typically feature larger hydraulic diameters compared to smaller trees (Anfodillo et al., 2006), which also translates into time series (Carrer et al., 2015). However, as shown in Buras et al. (2018) forest edge trees were in fact significantly shorter compared to interior trees (see Figure 2F in Buras et al., 2018), possibly due to a lower competition for light at the forest edge and thus a lower necessity to outcompete neighboring trees via apical growth or due to mechanical acclimation to a higher wind exposure at the forest edge (Chehab et al., 2009; Moulia et al., 2015). Given the positive link between hydraulic diameter and tree height, the finding of higher hydraulic diameters at the forest edge – where trees were shorter – even more points toward a hydraulic adjustment due to differing micro-climatic conditions.

4.3. Potential early warning indicators of tree dieback

Besides the comparison among groups over the whole investigated period, we want to stress the abrupt decline of several anatomical parameters for dying trees since the year 2012. In particular, latewood cell-wall thickness, mean ring density, earlywood hydraulic diameter and cell-wall reinforcement of dying trees abruptly declined in 2012 (Figures 3A,C,D,E), whereas earlywood cell-wall thickness declined in 2013. At the study site, the year of 2012 was characterized by a moderate drought (January–September SPEI = −1.3, see Supplementary Figure 4) which ranks eleventh among all local droughts since 1901. Moreover 2012 was preceded by the relatively dry year of 2011 (January–September SPEI = −1.1, see Supplementary Figure 4), potentially amplifying soil drought in case the soil water storage was not replenished in the winter 2011/2012. The comparably strong drought effects of 2012 are likely also reflected in the comparably high $\delta^{13}C$ values for all trees (Figure 2A). In context of how droughts evolve in Central Europe (e.g., Buras et al., 2020), the observed lag of earlywood cell wall thickness decline seems plausible. Because drought usually develops during the growing season and peaks in July–August, a time when earlywood formation is largely completed, the effects of drought on reduced photo-assimilate availability in 2012 did not strongly affect earlywood cell wall thickness. In contrast, the observed decline in earlywood hydraulic diameter already in 2012 may be considered an anatomical adjustment to the moderately dry conditions resulting from 2011. That is, low soil water potentials in spring 2012 hampered turgor-driven tracheid enlargement as has been shown for other sites before (Cabon et al., 2020). This possibly also explains the abrupt decline of earlywood hydraulic diameter of all edge trees in 2014 which was characterized by dry conditions (January–September SPEI = −1.1, see Supplementary Figure 4) as is reflected in higher $\delta^{13}C$ values in all trees. Therefore, the large decrease in earlywood hydraulic diameter for all edge trees in 2014 could be due to accumulated drought effects related to the plant available soil water over the period 2011–2014. It is important to stress, that this interpretation does not contradict our interpretation of an anatomical adjustment of the xylem to dry conditions on the longer term as formulated in section 4.2 and context of H4. That is, on the one hand the frequent, drought-induced reduction of stomatal conductance probably caused a shortage in photo-assimilates which in turn led to a more cost-efficient wood anatomy featuring thinner cell walls (reduced carbon investment) with wider lumina (more efficient sap-flow). On the other hand, overly dry conditions early in the growing season of 2012 and 2014 caused by soil-moisture related carry-over effects from the, respectively, previous year hampered cell enlargement due to a relatively low cell turgor. In conclusion, the observations of abruptly declining wood anatomical traits point toward potential early-warning indicators of tree dieback (Pellizzari et al., 2016). Moreover, our results suggest that carbon depletion goes hand in hand with an increase in hydraulic vulnerability, a pattern often seen in drought-induced tree mortality (Adams et al., 2017).

It is important to stress, that we cannot rule out effects of forest management on our results due to a lack of information on local management history. In fact, BAI time-series suggest a thinning-induced growth release of the forest interior around the year 2006 (Figure 1B). As a consequence, competition for water and light would be reduced. Yet, a possible thinning would likely also reduce competition of forest-edge trees, which however showed no growth release in that period, possibly due to detrimental drought effects counteracting a potential thinning effect. Independent of possible management activities around 2006, the time series under investigation showed systematic differences between edge and interior trees before 2006 and featured no abrupt shift of the investigated parameters around 2006. Thus, even if management had taken place, we believe related effects on the studied parameters to be statistically negligible. Yet, the weak negative trend in $\delta^{13}C$ observed for interior

trees (Figure 2A) might result from a slightly improved plant-water availability after 2006 due to a lower stand density.

5. Conclusion

Based on stable carbon isotope and quantitative wood anatomy measurements, our study sheds light on the mechanisms causing a higher drought-vulnerability of Scots pine in proximity to the forest edge. Higher $\delta^{13}C$ as well as lower cell-wall thickness and mean ring density at the edge suggest a downregulation of stomatal conductance, which not only increases the ^{13}C fraction in the xylem tissue but also results in a reduced availability of photo-assimilates and consequently thinner cell walls and narrower tree rings. Regarding the differentiation between live and dead trees growing at the forest edge, a lower cell-wall reinforcement indicates a higher likelihood of dead trees to have suffered from cavitation. This could be exacerbated by the larger earlywood hydraulic diameter if earlywood cells were to cavitate, as they contribute over-proportionally to water transport. These findings suggest wood anatomical traits to render a promising avenue for understanding spatial patterns of tree dieback. Yet, our explanation of the underlying causes for anatomical differences requires further investigation across environmental gradients and for various tree species.

Altogether, our findings highlight the necessity to emphasize on micro-climatic aspects in context of forest management operations. This is of particular importance under climate change, since forest edges are likely to suffer the most from an increasing frequency and intensity of severe droughts under climate change. Consequently, forest edges may be considered a hotspot and potential early-warning indicator for species-specific, climate-change induced forest decline. To counteract potential positive feedback loops of edge dieback and increase forests' resilience to climate change, forest management could aim to establish buffer zones at forest-edges where more drought-resilient tree species are planted.

Data availability statement

The raw data supporting the conclusions of this article will be made available by the authors, without undue reservation.

Author contributions

AB collected the samples, analyzed the data, and drafted the manuscript. RR conducted the stable carbon isotope lab-work. MF, PF, and JL conducted the quantitative wood anatomy lab-work. AB, AG, AM, AR, GA, and KT designed the methodological approach. All authors commented on and approved the manuscript prior to submission.

Acknowledgments

We like to thank Loïc Schneider from the WSL Dendrosciences research group for assistance with cellulose extraction and Manuela Oettli for isotopic MS analyses. AG acknowledges financial support from SNF (310030_189109). We thank the reviewers and handling editor for their valuable suggestions to improve our manuscript.

Conflict of interest

The authors declare that the research was conducted in the absence of any commercial or financial relationships that could be construed as a potential conflict of interest.

Publisher's note

Supplementary material

The Supplementary material for this article can be found online at: https://www.frontiersin.org/articles/10.3389/ffgc.2023.1233052/full#supplementary-material

References

Adams, H. D., Zeppel, M. J. B., Anderegg, W. R. L., Hartmann, H., Landhäusser, S. M., Tissue, D. T., et al. (2017). A multi-species synthesis of physiological mechanisms in drought-induced tree mortality. *Nat. Ecol. Evol.* 1, 1285–1291. doi: 10.1038/s41559-017-0248-x

Allen, C. D., Breshears, D. D., and McDowell, N. G. (2015). On underestimation of global vulnerability to tree mortality and forest die-off from hotter drought in the Anthropocene. *Ecosphere* 6, art129–art155. doi: 10.1890/ES15-00203.1

Allen, C. D., Macalady, A. K., Chenchouni, H., Bachelet, D., McDowell, N., Vennetier, M., et al. (2010). A global overview of drought and heat-induced tree mortality reveals emerging climate change risks for forests. *For. Ecol. Manag.* 259, 660–684. doi: 10.1016/j.foreco.2009.09.001

Anfodillo, T., Carraro, V., Carrer, M., Fior, C., and Rossi, S. (2006). Convergent tapering of xylem conduits in different woody species. *New Phytol.* 169, 279–290. doi: 10.1111/j.1469-8137.2005.01587.x

Beguería, S., and Vicente-Serrano, S. M. (2013). SPEI: calculation of the standardised precipitation-evapotranspiration index. *R pac. ver.* 1:6.

Björklund, J., Seftigen, K., Schweingruber, F., Fonti, P., von Arx, G., Bryukhanova, M. V., et al. (2017). Cell size and wall dimensions drive distinct variability of earlywood and latewood density in northern hemisphere conifers. *New Phytol.* 216, 728–740. doi: 10.1111/nph.14639

Björklund, J., von Arx, G., Nievergelt, D., Wilson, R., Van den Bulcke, J., Günther, B., et al. (2019). Scientific merits and analytical challenges of tree-ring densitometry. *Rev. Geophys.* 57, 1224–1264. doi: 10.1029/2019RG000642

Bonan, G. B. (2008). Forests and climate change: forcings, feedbacks, and the climate benefits of forests. *Science* 320, 1444–1449. doi: 10.1126/science.1155121

Brandes, E., Kodama, N., Whittaker, K., Weston, C., Rennenberg, H., Keitel, C., et al. (2006). Short-term variation in the isotopic composition of organic matter allocated from the leaves to the stem of *Pinus sylvestris*: effects of photosynthetic and postphotosynthetic carbon isotope fractionation. *Glob. Chang. Biol.* 12, 1922–1939. doi: 10.1111/j.1365-2486.2006.01205.x

Brienen, R. J. W., Phillips, O. L., Feldpausch, T. R., Gloor, E., Baker, T. R., Lloyd, J., et al. (2015). Long-term decline of the Amazon carbon sink. *Nature* 519, 344–348. doi: 10.1038/nature14283

Bunn, A. G. (2008). A dendrochronology program library in R (dplR). *Dendrochronologia* 26, 115–124. doi: 10.1016/j.dendro.2008.01.002

Buras, A. (2017). A comment on the expressed population signal. *Dendrochronologia* 44, 130–132. doi: 10.1016/j.dendro.2017.03.005

Buras, A., (2022). *dendRolAB Analytical tools for tree-ring data*. https://github.com/AllanBuras/dendRolAB

Buras, A., and Menzel, A. (2019). Projecting tree species composition changes of European forests for 2061–2090 under RCP 4.5 and RCP 8.5 scenarios. *Front. Plant Sci.* 9:1986. doi: 10.3389/fpls.2018.01986

Buras, A., Rammig, A., and Zang, C. S. (2020). Quantifying impacts of the 2018 drought on European ecosystems in comparison to 2003. *Biogeosciences* 17, 1655–1672. doi: 10.5194/bg-17-1655-2020

Buras, A., Rammig, A., and Zang, C. S. (2021). The European Forest condition monitor: using remotely sensed Forest greenness to identify hot spots of Forest decline. *Front. Plant Sci.* 12:2355. doi: 10.3389/fpls.2021.689220

Buras, A., Schunk, C., Zeiträg, C., Herrmann, C., Kaiser, L., Lemme, H., et al. (2018). Are scots pine forest edges particularly prone to drought-induced mortality? *Environ. Res. Lett.* 13:025001. doi: 10.1088/1748-9326/aaa0b4

Buras, A., Van Der Maaten-Theunissen, M., Van Der Maaten, E., Ahlgrimm, S., Hermann, P., Simard, S., et al. (2016). Tuning the voices of a choir: detecting ecological gradients in time-series populations. *PLoS One* 11:e0158346. doi: 10.1371/journal.pone.0158346

Buras, A., and Wilmking, M. (2015). Correcting the calculation of Gleichläufigkeit. *Dendrochronologia* 34, 29–30. doi: 10.1016/j.dendro.2015.03.003

Cabon, A., Fernández-de-Uña, L., Gea-Izquierdo, G., Meinzer, F. C., Woodruff, D. R., Martínez-Vilalta, J., et al. (2020). Water potential control of turgor-driven tracheid enlargement in scots pine at its xeric distribution edge. *New Phytol.* 225, 209–221. doi: 10.1111/nph.16146

Cabon, A., Kannenberg, S. A., Arain, A., Babst, F., Baldocchi, D., Belmecheri, S., et al. (2022). Cross-biome synthesis of source versus sink limits to tree growth. *Science* 376, 758–761. doi: 10.1126/science.abm4875

Cailleret, M., Jansen, S., Robert, E. M. R., Desoto, L., Aakala, T., Antos, J. A., et al. (2017). A synthesis of radial growth patterns preceding tree mortality. *Glob. Change Biol.* 23, 1675–1690. doi: 10.1111/gcb.13535

Carrer, M., von Arx, G., Castagneri, D., and Petit, G. (2015). Distilling allometric and environmental information from time series of conduit size: the standardization issue and its relationship to tree hydraulic architecture. *Tree Physiol.* 35, 27–33. doi: 10.1093/treephys/tpu108

Chehab, E. W., Eich, E., and Braam, J. (2009). Thigmomorphogenesis: a complex plant response to mechano-stimulation. *J. Exp. Bot.* 60, 43–56. doi: 10.1093/jxb/ern315

Chen, J., Franklin, J. F., and Spies, T. A. (1993). Contrasting microclimates among clearcut, edge, and interior of old-growth Douglas-fir forest. *Agric. For. Meteorol.* 63, 219–237. doi: 10.1016/0168-1923(93)90061-L

Ciais, P., Reichstein, M., Viovy, N., Granier, A., Ogée, J., Allard, V., et al. (2005). Europe-wide reduction in primary productivity caused by the heat and drought in 2003. *Nature* 437, 529–533. doi: 10.1038/nature03972

De Frenne, P., Lenoir, J., Luoto, M., Scheffers, B. R., Zellweger, F., Aalto, J., et al. (2021). Forest microclimates and climate change: importance, drivers and future research agenda. *Glob. Chang. Biol.* 27, 2279–2297. doi: 10.1111/gcb.15569

Denne, M. P. (1989). Definition of latewood according to Mork (1928). *IAWA J.* 10, 59–62. doi: 10.1163/22941932-90001112

Eckstein, D., and Bauch, J. (1969). Beitrag zur Rationalisierung eines dendrochronologischen Verfahrens und zur Analyse seiner Aussagesicherheit. *Forstwissenschaftliches Centralblatt* 88, 230–250. doi: 10.1007/BF02741777

Eilmann, B., Buchmann, N., Siegwolf, R., Saurer, M., Cherubini, P., and Rigling, A. (2010). Fast response of scots pine to improved water availability reflected in tree-ring width and δ13C. *Plant Cell Environ.* 33, 1351–1360. doi: 10.1111/j.1365-3040.2010.02153.x

Eilmann, B., Zweifel, R., Buchmann, N., Fonti, P., and Rigling, A. (2009). Drought-induced adaptation of the xylem in scots pine and pubescent oak. *Tree Physiol.* 29, 1011–1020. doi: 10.1093/treephys/tpp035

Estreguil, C., Caudullo, G., de Rigo, D., and San-Miguel-Ayanz, J. (2013). Forest landscape in Europe: pattern, fragmentation and connectivity. *Eur Sci. Tech. Res.* 25717. doi: 10.2788/77842

Farquhar, G. D., O'Leary, M. H., and Berry, J. A. (1982). On the relationship between carbon isotope discrimination and the intercellular carbon dioxide concentration in leaves. *Funct. Plant Biol.* 9, 121–137. doi: 10.1071/PP9820121

Galiano, L., Timofeeva, G., Saurer, M., Siegwolf, R., Martínez-Vilalta, J., Hommel, R., et al. (2017). The fate of recently fixed carbon after drought release: towards unravelling C storage regulation in Tilia platyphyllos and *Pinus sylvestris*. *Plant Cell Environ.* 40, 1711–1724. doi: 10.1111/pce.12972

Gärtner, H., and Schweingruber, F.H., (2013). *Microscopic preparation techniques for plant stem analysis*. Verlag Dr. Kessel, Remagen.

Gessler, A., Cailleret, M., Joseph, J., Schönbeck, L., Schaub, M., Lehmann, M., et al. (2018). Drought induced tree mortality–a tree-ring isotope based conceptual model to assess mechanisms and predispositions. *New Phytol.* 219, 485–490. doi: 10.1111/nph.15154

Giuggiola, A., Bugmann, H., Zingg, A., Dobbertin, M., and Rigling, A. (2013). Reduction of stand density increases drought resistance in xeric scots pine forests. *For. Ecol. Manag.* 310, 827–835. doi: 10.1016/j.foreco.2013.09.030

Giuggiola, A., Ogée, J., Rigling, A., Gessler, A., Bugmann, H., and Treydte, K. (2016). Improvement of water and light availability after thinning at a xeric site: which matters more? A dual isotope approach. *New Phytol.* 210, 108–121. doi: 10.1111/nph.13748

Giuggiola, A., Zweifel, R., Feichtinger, L. M., Vollenweider, P., Bugmann, H., Haeni, M., et al. (2018). Competition for water in a xeric forest ecosystem–effects of understory removal on soil micro-climate, growth and physiology of dominant scots pine trees. *For. Ecol. Manag.* 409, 241–249. doi: 10.1016/j.foreco.2017.11.002

Grote, R., Gessler, A., Hommel, R., Poschenrieder, W., and Priesack, E. (2016). Importance of tree height and social position for drought-related stress on tree growth and mortality. *Trees* 30, 1467–1482. doi: 10.1007/s00468-016-1446-x

Guérin, M., von Arx, G., Martin-Benito, D., Andreu-Hayles, L., Griffin, K. L., McDowell, N. G., et al. (2020). Distinct xylem responses to acute vs prolonged drought in pine trees. *Tree Physiol.* 40, 605–620. doi: 10.1093/treephys/tpz144

Hacke, U. G., and Sperry, J. S. (2001). Functional and ecological xylem anatomy. *Perspect. Plant Ecol. Evol. Syst.* 4, 97–115. doi: 10.1078/1433-8319-00017

Hacke, U. G., Sperry, J. S., Pockman, W. T., Davis, S. D., and McCulloh, K. A. (2001). Trends in wood density and structure are linked to prevention of xylem implosion by negative pressure. *Oecologia* 126, 457–461. doi: 10.1007/s004420100628

Harris, I., Osborn, T. J., Jones, P., and Lister, D. (2020). Version 4 of the CRU TS monthly high-resolution gridded multivariate climate dataset. *Sci. Data* 7:109. doi: 10.1038/s41597-020-0453-3

Hentschel, R., Rosner, S., Kayler, Z. E., Andreassen, K., Børja, I., Solberg, S., et al. (2014). Norway spruce physiological and anatomical predisposition to dieback. *For. Ecol. Manag.* 322, 27–36. doi: 10.1016/j.foreco.2014.03.007

Jump, A. S., Ruiz-Benito, P., Greenwood, S., Allen, C. D., Kitzberger, T., Fensham, R., et al. (2017). Structural overshoot of tree growth with climate variability and the global spectrum of drought-induced forest dieback. *Glob. Chang. Biol.* 23, 3742–3757. doi: 10.1111/gcb.13636

Klein, T. (2014). The variability of stomatal sensitivity to leaf water potential across tree species indicates a continuum between isohydric and anisohydric behaviours. *Funct. Ecol.* 28, 1313–1320. doi: 10.1111/1365-2435.12289

Klein, T., Shpringer, I., Fikler, B., Elbaz, G., Cohen, S., and Yakir, D. (2013). Relationships between stomatal regulation, water-use, and water-use efficiency of two coexisting key Mediterranean tree species. *For. Ecol. Manag.* 302, 34–42. doi: 10.1016/j.foreco.2013.03.044

Klesse, S., Wohlgemuth, T., Meusburger, K., Vitasse, Y., von Arx, G., Lévesque, M., et al. (2022). Long-term soil water limitation and previous tree vigor drive local variability of drought-induced crown dieback in *Fagus sylvatica*. *Sci. Total Environ.* 851:157926. doi: 10.1016/j.scitotenv.2022.157926

Klisz, M., Buras, A., Sass-Klaassen, U., Puchalka, R., Koprowski, M., and Ukalska, J. (2019). Limitations at the limit? Diminishing of genetic effects in Norway spruce provenance trials. *Front. Plant Sci.* 10:306. doi: 10.3389/fpls.2019.00306

Kohler, M., Sohn, J., Nägele, G., and Bauhus, J. (2010). Can drought tolerance of Norway spruce be increased through thinning? *Eur. J. Forest. Res.* 129, 1109–1118. doi: 10.1007/s10342-010-0397-9

Laumer, W., Andreu, L., Helle, G., Schleser, G. H., Wieloch, T., and Wissel, H. (2009). A novel approach for the homogenization of cellulose to use micro-amounts for stable isotope analyses. *Rapid Commun. Mass Spectrom.* 23, 1934–1940. doi: 10.1002/rcm.4105

Laurance, W. F., and Williamson, G. B. (2001). Positive feedbacks among forest fragmentation, drought, and climate change in the Amazon. *Conserv. Biol.* 15, 1529–1535. doi: 10.1046/j.1523-1739.2001.01093.x

Lévesque, M., Saurer, M., Siegwolf, R., Eilmann, B., Brang, P., Bugmann, H., et al. (2013). Drought response of five conifer species under contrasting water availability suggests high vulnerability of Norway spruce and European larch. *Glob. Change Biol.* 19, 3184–3199. doi: 10.1111/gcb.12268

Loader, N. J., McCarroll, D., Gagen, M., Robertson, I., and Jalkanen, R. (2007). Extracting climatic information from stable isotopes in tree rings. *Terrestrial Ecology*, 1, 25–48.

López, R., Cano, F. J., Rodríguez-Calcerrada, J., Sangüesa-Barreda, G., Gazol, A., Camarero, J. J., et al. (2021). Tree-ring density and carbon isotope composition are early-warning signals of drought-induced mortality in the drought tolerant Canary Island pine. *Agric. For. Meteorol.* 310:108634. doi: 10.1016/j.agrformet.2021.108634

Mann, D., Gohr, C., Blumroeder, J. S., and Ibisch, P. L. (2023). Does fragmentation contribute to the forest crisis in Germany? *Front. For. Glob. Change* 6:1. doi: 10.3389/ffgc.2023.1099460

Matlack, G. R. (1993). Microenvironment variation within and among forest edge sites in the eastern United States. *Biol. Conserv.* 66, 185–194. doi: 10.1016/0006-3207(93)90004-K

Meeussen, C., Govaert, S., Vanneste, T., Bollmann, K., Brunet, J., Calders, K., et al. (2021). Microclimatic edge-to-interior gradients of European deciduous forests. *Agric. For. Meteorol.* 311:108699. doi: 10.1016/j.agrformet.2021.108699

Moulia, B., Coutand, C., and Julien, J.-L. (2015). Mechanosensitive control of plant growth: bearing the load, sensing, transducing, and responding. *Front. Plant Sci.* 6:52. doi: 10.3389/fpls.2015.00052

Pellizzari, E., Camarero, J. J., Gazol, A., Sangüesa-Barreda, G., and Carrer, M. (2016). Wood anatomy and carbon-isotope discrimination support long-term hydraulic deterioration as a major cause of drought-induced dieback. *Glob. Change Biol.* 22, 2125–2137. doi: 10.1111/gcb.13227

Petrucco, L., Nardini, A., von Arx, G., Saurer, M., and Cherubini, P. (2017). Isotope signals and anatomical features in tree rings suggest a role for hydraulic strategies in diffuse drought-induced die-back of *Pinus nigra*. *Tree Physiol.* 37, 523–535. doi: 10.1093/treephys/tpx031

Prendin, A. L., Mayr, S., Beikircher, B., von Arx, G., and Petit, G. (2018). Xylem anatomical adjustments prioritize hydraulic efficiency over safety as Norway spruce trees grow taller. *Tree Physiol.* 38, 1088–1097. doi: 10.1093/treephys/tpy065

Prendin, A. L., Petit, G., Carrer, M., Fonti, P., Björklund, J., and von Arx, G. (2017). New research perspectives from a novel approach to quantify tracheid wall thickness. *Tree Physiol.* 37, 976–983. doi: 10.1093/treephys/tpx037

R Core Team, (2022). *R: a language and environment for statistical computing*. R Foundation for Statistical Computing, Vienna.

Rehschuh, R., Mette, T., Menzel, A., and Buras, A. (2017). Soil properties affect the drought susceptibility of Norway spruce. *Dendrochronologia* 45, 81–89. doi: 10.1016/j.dendro.2017.07.003

Rosner, S., Světlík, J., Andreassen, K., Børja, I., Dalsgaard, L., Evans, R., et al. (2016). Novel hydraulic vulnerability proxies for a boreal conifer species reveal that opportunists may have lower survival prospects under extreme climatic events. *Front. Plant Sci.* 7:831. doi: 10.3389/fpls.2016.00831

Seidel, H., and Menzel, A. (2016). Above-ground dimensions and acclimation explain variation in drought mortality of scots pine seedlings from various provenances. *Front. Plant Sci.* 7:1014. doi: 10.3389/fpls.2016.01014

Seidel, H., Schunk, C., Matiu, M., and Menzel, A. (2016). Diverging drought resistance of scots pine provenances revealed by infrared thermography. *Front. Plant Sci.* 7:1247. doi: 10.3389/fpls.2016.01247

Sherich, K., Pocewicz, A., and Morgan, P. (2007). Canopy characteristics and growth rates of ponderosa pine and Douglas-fir at long-established forest edges. *Can. J. For. Res.* 37, 2096–2105. doi: 10.1139/X07-105

Sperry, J. S. (2003). Evolution of water transport and xylem structure. *Int. J. Plant Sci.* 164, S115–S127. doi: 10.1086/368398

Thornthwaite, C. W. (1948). An approach toward a rational classification of climate. *Geogr. Rev.* 38, 55–94. doi: 10.2307/210739

Tyree, M. T., and Zimmermann, M. H. (2002). "Conducting units: tracheids and vessels" in *Xylem structure and the ascent of sap* (Berlin, Heidelberg: Springer), 1–25.

Vicente-Serrano, S. M., Beguería, S., and López-Moreno, J. I. (2009). A multiscalar drought index sensitive to global warming: the standardized precipitation evapotranspiration index. *J. Clim.* 23, 1696–1718. doi: 10.1175/2009JCLI2909.1

von Arx, G., and Carrer, M. (2014). ROXAS – a new tool to build centuries-long tracheid-lumen chronologies in conifers. *Dendrochronologia* 32, 290–293. doi: 10.1016/j.dendro.2013.12.001

von Arx, G., Crivellaro, A., Prendin, A. L., Čufar, K., and Carrer, M. (2016). Quantitative wood anatomy—practical guidelines. *Front. Plant Sci.* 7:781. doi: 10.3389/fpls.2016.00781

Walentowski, H., Falk, W., Mette, T., Kunz, J., Bräuning, A., Meinardus, C., et al. (2017). Assessing future suitability of tree species under climate change by multiple methods: a case study in southern Germany. *Ann. For. Res.* 60, 101–126. doi: 10.15287/afr.2016.789

Wigley, T. M. L., Briffa, K. R., and Jones, P. D. (1984). On the average value of correlated time series, with applications in dendroclimatology and hydrometeorology. *J. Climate Appl. Meteor.* 23, 201–213. doi: 10.1175/1520-0450(1984)023<0201:OTAVOC>2.0.CO;2

Young, A., and Mitchell, N. (1994). Microclimate and vegetation edge effects in a fragmented podocarp-broadleaf forest in New Zealand. *Biol. Conserv.* 67, 63–72. doi: 10.1016/0006-3207(94)90010-8